ELSEVIER

Journal of Photochemistry and Photobiology A: Chemistry 124 (1999) 101–112

Journal of Photochemistry and Photobiology A:Chemistry

A box model of the photolysis of methane at 123.6 and 147 nm—comparison between model and experiment

N.S. Smith, F. Raulin*

Laboratoire Interuniversitaire des Systèmes Atmosphériques, Université Paris 12, 61, av. du Général de Gaulle, 94010 Créteil Cedex, France

Received 18 January 1999; received in revised form 25 March 1999; accepted 25 March 1999

Abstract

We have taken existing experimental measurements of the chemical evolution of samples of CH_4, subjected to photolysis at 123.6 and 147 nm. We have compared these measurements with the theoretical predictions of a photochemical box model using three different reaction schemes with the ultimate aim of developing a scheme valid for all values of temperature, pressure and photolysis wavelength. The laboratory results seem to have been influenced by an experimental wall effect leading to loss of H atoms. We propose a scheme of reactions that seems the most robust under conditions of low temperatures and pressures, required for the modelling of planetary atmospheres, such as that of Titan, and of the interstellar medium. It appears that there is still some uncertainty in the mechanism of production of C_2H_2 under the conditions of the two laboratory experiments studied. There is also a need to investigate the sensitivity of the results of such photochemical schemes to the values of rate constants, absorption cross sections and quantum yields used.

Keywords: Modelling; Photolysis; Methane; Hydrocarbons; Titan; Saturn; Jupiter

1. Introduction

The gas-phase chemistry of simple hydrocarbons is complex and still far from fully understood. In order to model this chemistry, in environments as diverse as hydrocarbon flames and the atmospheres of Jupiter [1], Saturn [2] and its largest satellite, Titan [3–6], we require kinetic data for a large number of reactions [7–12]. On account of the difficulty of determining this data in the laboratory, particularly under the conditions of pressure and temperature required for these models, many rate constants are poorly known or have yet to be determined. In addition, measurements of the products and quantum yields for hydrocarbon photolyses are also scarce.

In order to better constrain these data, and hence increase our understanding of hydrocarbon chemistry, we must assess how well the data currently available can explain the experimental observations of the behaviour of non-trivial systems. Therefore, we have compared the results of CH_4 photolyses performed in the laboratory at 123.6 nm [13] and 147 nm [14] with the predictions of a theoretical box model. We have adapted two existing photochemical schemes [4,5] to the temperatures, pressures and photolysis wavelengths of these two laboratory experiments. We have also judiciously constructed, using the most recent chemical literature, our own scheme containing the photolysis of 10 compounds and 72 subsequent radical reactions. The three schemes are compared in Appendix A. The most obvious difference between our scheme and the two existing ones is the description of CH_4 dissociation; we take the quantum yields from Smith and Raulin [15], while Yung et al. and Toublanc et al. took the values of Slanger [16]. There are also many minor differences between the schemes that arise from the uncertainties in the kinetic data used. The markedly different behaviour we have found for these three models has led us to investigate the propagation of imprecisions in the kinetic data to the model results. This will be described in a subsequent paper.

2. Experimental data

Hellner irradiated 10 Torr of CH_4 at 123.6 nm by use of a Kr lamp. The methane sample was placed in a Pyrex bulb of 700 cm^3 volume. The flux of photons traversing the Kr lamp MgF_2 window was determined by NO actinometry, to be 5×10^{15} photons s^{-1}. Experiments were carried out at room

*Corresponding author. Tel.: +33-1-45-17-15-60; fax: +33-1-45-17-15-64; e-mail: raulin@lisa.univ-paris12.fr

1010-6030/99/$ – see front matter
PII: S1010-6030(99)00074-X

temperature (300 K) and liquid nitrogen temperature (77 K) for varying irradiation times up to 60 min, and the resulting gas mixture was analysed by gas chromatography. In this way, the concentrations of C_2H_2, C_2H_4, C_2H_6, C_3H_6 and C_3H_8 were quantified after 5, 10, 15, 20, 30 and 60 min of photolysis.

Bossard performed similar experiments at 147 nm using a Xe lamp. The Pyrex sample cell used was cylindrical in shape with a volume of 500 cm^3 and a length of 35 cm. The number of photons passing through the MgF_2 window of the Xe lamp was calculated by CO_2 actinometry, assuming a quantum yield of 1 for conversion to CO. Experiments were carried out, at room temperature, for CH_4 pressures of 6 Torr (eight different irradiation times, up to ca. 20 min) and 9 Torr (four different times, up to 60 min). The evolution of C_2H_2, C_2H_4, C_2H_6 and C_3H_8 concentrations was recorded, also by gas chromatography.

3. Photochemical model

We have used our three chemical schemes in the FACSIMILE chemical reaction modeller [17], to simulate the two laboratory experiments of Hellner and Bossard outlined above. We have considered species up to C_4H_4 with any heavier molecules produced being removed in the form of polyyne species ($C_{2n}H_2$) or soot and no longer participating in the model.

3.1. Photolysis rates

The photolysis rate of species, i, is described in terms of its concentration, C_i, as

$$\frac{-\mathrm{d}C_i}{\mathrm{d}t} = J_i \times C_i$$

where J_i is the photodissociation coefficient for species i, in units of s^{-1}. Under the laboratory conditions of Hellner and Bossard, the amount of radiation absorbed by the sample is not always small compared to the total flux. Therefore, we cannot calculate J_i simply, at a given wavelength, as

$$J_i = \Phi_i \times \sigma_i \times I$$

where Φ_i is the total primary quantum yield of dissociation of species i ($\Phi_i \leq 1$), σ_i the absorption cross section, and I the flux of the light source in photons $cm^{-2}\ s^{-1}$. We have to calculate J_i as follows:

The actinometry measurements performed by the authors give the total number of photons emitted by the lamp that enter the cell, I(in). We can calculate, from the Beer–Lambert Law, the number of photons absorbed by the sample, I(abs), as

$$I(\mathrm{abs}) = I(\mathrm{in}) - I(\mathrm{out}) \equiv I(\mathrm{in}) \times \left(1 - \exp\left(-\sum \sigma_i \times C_i \times L\right)\right)$$

where L is the optical path length through the cell. If the cell contains only one absorbing species, we can write that

$$\frac{-\mathrm{d}C_i}{\mathrm{d}t} = \Phi_i \times \frac{I(\mathrm{abs})}{V}$$

where V is the volume of the cell. If the cell contains more than one absorber, then we must also add a term f_i, the fraction of the photons absorbed by the mixture which is absorbed by species i. We can simply define this factor as

$$f_i = \frac{\sigma_i \times C_i}{\sum(\sigma_i \times C_i)}$$

Therefore, we can equate the two expressions for $-\mathrm{d}C_i/\mathrm{d}t$ and calculate J_i to be

$$J_i = \frac{\Phi_i \times I(\mathrm{abs}) \times f_i}{(C_i \times V)}$$

This is an 'effective' J_i that can be used in the dimensionless box model, but which takes into account the transmission of the radiation through the sample. The values of σ_i and Φ_i at 123.6 and 147 nm are listed in Appendix A. We note that no accurate experimental value for the very small absorption cross section of CH_4 at 147 nm exists, hence we assume a value of 1×10^{-20} cm^2 [18].

3.2. Thermal reaction rates

For a bimolecular reaction between two species i and j, we define the rate as

$$\frac{-\mathrm{d}C_i}{\mathrm{d}t} = k_{i,j} \times C_i \times C_j$$

where $k_{i,j}$ is the bimolecular rate constant, in $cm^3\ s^{-1}$, defined for each reaction in the photochemical scheme. However, some of the reactions require a collision with a third body in order to stabilise the product. In these cases, we define an effective bimolecular rate constant as

$$k = \frac{k_0 \times k_\infty \times M}{k_\infty + (k_0 \times M)}$$

where k_0 ($cm^6\ s^{-1}$) and k_∞ ($cm^3\ s^{-1}$) are, respectively, the rate coefficients in the low and high pressure limits and M (molecules cm^{-3}) is the concentration of collision partners, assumed to be equal to the total number density.

Values for k, k_0 and k_∞ are given in Appendix A. We first took the recommended values quoted in review articles [7–9], when such values existed. Otherwise, we took well-trusted laboratory data, when available. However, for some reactions, no data exists and we have had to estimate the rate constants by comparison with other chemically similar reactions.

4. Results and discussion

4.1. CH_4 photolysis at 123.6 nm

We have modelled this experiment, for an initial pressure of 10 Torr of CH_4 (3.2×10^{17} molecules cm^{-3}) at two different temperatures, namely 300 K and 77 K. The results

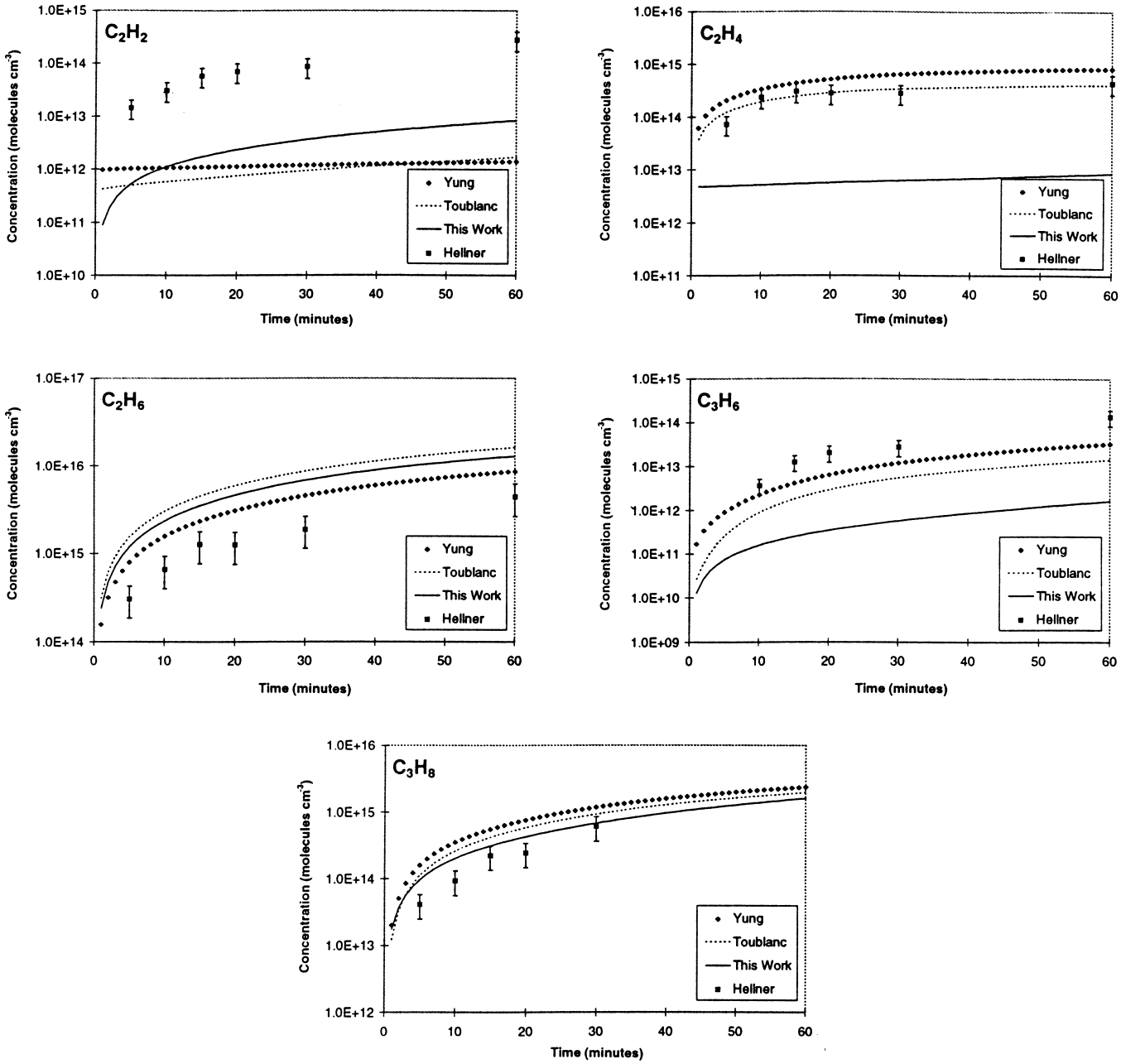

Fig. 1. Comparison of Hellner's results at 300 K (with error bars) with the photochemical schemes of Yung, Toublanc and our own model.

are shown in Figs. 1 and 2, respectively. The indicated error bars of 40% shown in the experimental results are those estimated by the author [13], and arise from uncertainties in the flux of the Kr lamp used and the quantitative analysis by gas chromatography. Even considering these experimental uncertainties, we can clearly see some strong disagreements between these results and the predictions of the different box models.

Our models that use the schemes of Yung and Toublanc manage to reproduce the observed evolutions at 300 K fairly well for all but C_2H_2, but are much less satisfactory at 77 K. In addition, they both predict concentrations of C_3H_4 (both isomers) significantly higher than those of C_3H_6 and C_2H_2 at both temperatures. The gas-chromatography technique, used by Hellner to quantify the hydrocarbon products, should have a similar sensitivity to all C_3 hydrocarbons. Unless C_3H_4 was co-eluted in the chromatographic conditions used by Hellner, its concentration was much lower than those of the other C_3 hydrocarbons. This raises doubts about the accuracy of the chemical schemes used in these two models, particularly with respect to C_3 compounds. A comparison of C_3H_4 concentrations predicted by the three chemical schemes is shown in Table 1.

On the other hand, our photochemical scheme gives, by far, the poorest agreement with the experimental data at 300 K, particularly for C_2H_4 and C_3H_6, but it fits the

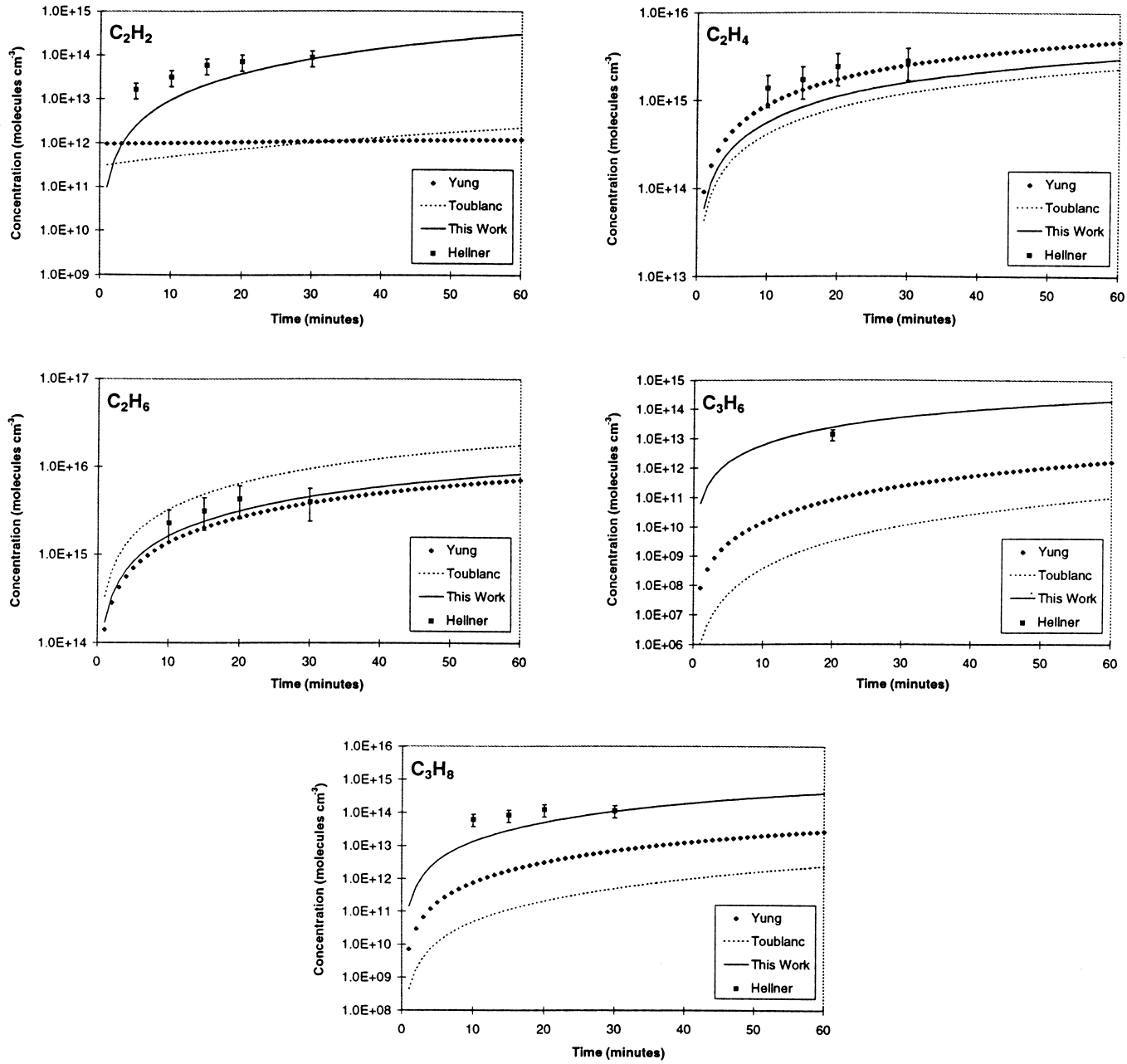

Fig. 2. Comparison of Hellner's results at 77 K (with error bars) with the photochemical schemes of Yung, Toublanc and our own model.

experimental data at 77 K remarkably well. This is surprising, as the kinetic rate constants that we have used have usually been determined at, or above, room temperature. We would, therefore, expect the model to be more trustworthy at 300 K than at 77 K, when extrapolation of rate constant values is necessary. Also, our model successfully predicts the low concentrations of C_3H_4 isomers, coherent with their non-detection in the experiment. However, to understand the differences between the three models at 300 K, and at 77 K, we shall look in more detail at the differences in the chemical schemes employed.

At 123.6 nm, the absorption cross sections of all major species in the mixture are of comparable magnitude, and hence, even after 60 min, more than 95% of the radiation absorbed leads to dissociation of CH_4, due to its much larger concentration. Hence, the radicals CH_3, $^1CH_2$, $^3CH_2$, CH, and H must play important roles in each model. In all the three chemical schemes, the production of CH is a minor process, and any $^1CH_2$ produced is rapidly converted to CH_3 or $^3CH_2$ through interaction with CH_4. We also find that the concentration of CH_3 is similar in all three models, and, as its principal loss is through self-recombination, this explains the similar forms for the C_2H_6 curves.

Therefore, the concentrations of the species C_2H_2, C_2H_4 and C_3H_6 are principally controlled by reactions involving either $^3CH_2$ or H. Our scheme produces considerably more

Table 1
Comparison of predicted C_3H_4 concentrations

Time (min)	Yung scheme		Toublanc scheme		This work	
	CH_3C_2H	CH_2CCH_2	CH_3C_2H	CH_2CCH_2	CH_3C_2H	CH_2CCH_2
123.6 nm						
2	3.9×10^{13}	2.7×10^{13}	4.2×10^{12}	7.0×10^{12}	1.0×10^{9}	1.0×10^{9}
20	4.7×10^{14}	1.7×10^{14}	8.6×10^{13}	5.0×10^{13}	3.4×10^{9}	3.4×10^{9}
60	1.5×10^{15}	3.6×10^{14}	3.8×10^{14}	1.4×10^{14}	1.1×10^{10}	1.2×10^{10}
147 nm						
2	1.6×10^{13}	1.2×10^{13}	3.5×10^{12}	7.2×10^{12}	2.6×10^{10}	3.2×10^{10}
20	2.1×10^{14}	1.7×10^{14}	1.4×10^{14}	1.0×10^{14}	5.9×10^{12}	5.2×10^{12}
60	3.3×10^{14}	2.5×10^{14}	3.4×10^{14}	2.0×10^{14}	1.2×10^{13}	1.1×10^{13}

atomic hydrogen, due to our choice of CH_4 dissociation quantum yields, and at 300 K, there is ca. 100 times more H in our model than in the others. Thus, both C_2H_2 and C_2H_4 react principally with H, while in the models of Yung and Toublanc, their reactions with $^3CH_2$ are more important. As our model agrees well with the data at 77 K and in predicting low concentrations of C_3H_4 isomers, we have tried to identify why our fit is poor at 300 K. We have, therefore, adapted our standard model in three ways to make models A, B and C, which are described below. The concentrations calculated by models A, B and C, and our standard model, are compared to the experimental results of Hellner at 300 K, in Fig. 3. All species show significant variations between the different models, except C_2H_6 which varies little and thus is not shown.

4.1.1. Model A

As our standard model underestimates the concentration of C_2H_4, we assume that the principal loss of this species, through reaction with H atoms, has been overestimated. In model A we have reduced the $C_2H_4 + H$ rate constant by a factor of 100 and it fits the experimental data remarkably well, except for C_2H_2 (see Fig. 3). To explain the C_2H_2 concentration, we would need to decrease the rate of $C_2H_2 + H$, also by a factor of ca. 100. In a recent review [8], the rate constants for $C_2H_4 + H$ and $C_2H_2 + H$ were

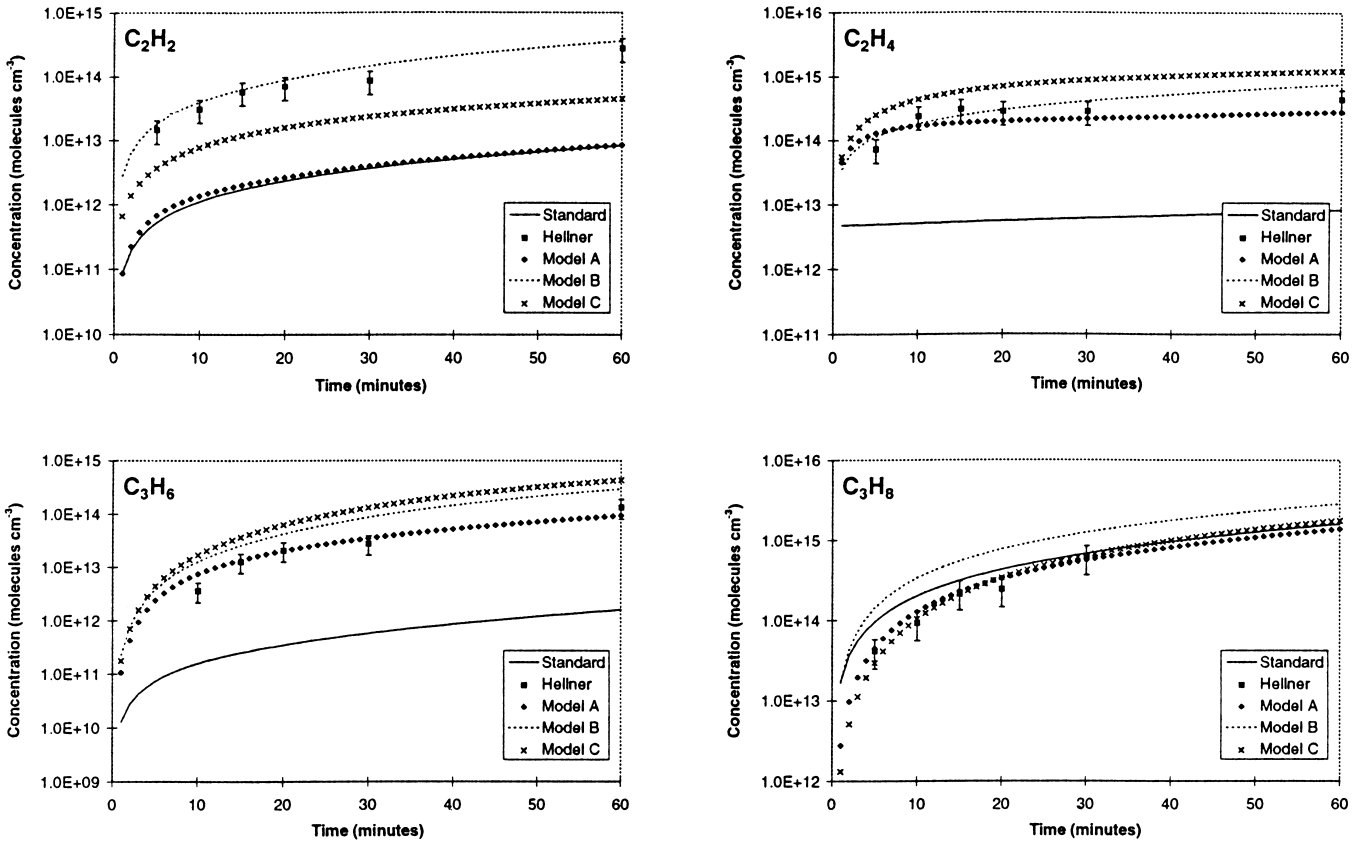

Fig. 3. Comparison of our models A, B and C (see text for details) with our standard model and the experimental data of Hellner (with error bars).

both considered to be accurate, at 300 K, to within about a factor of two. Therefore, it is more probable that our standard model simply overestimates the concentration of H atoms by two orders of magnitude. This implies that either the H atom production is too great or that H atom loss processes are missing.

4.1.2. Model B

Here, we assume that our standard model overpredicts the production of H atoms. The principal source of H atoms is the direct photolysis of CH_4, with a quantum yield of 0.47. In model B, as in the models of Yung and Toublanc, we have defined $^1CH_2 + H_2$ as the only product branch available at 123.6 nm, thus reducing the quantum yield of H atoms to zero. Such a scheme for CH_4 photolysis would be more coherent with early studies of this process at 123.6 nm, that determined a ratio of primary production of $^1CH_2/CH_3$ of 5.7 [19]. The influence of changing the details of CH_4 photolysis is highlighted by comparing the results of Model B with our standard model. Model B fits the observations of C_2H_2 and C_2H_4 well, but can not explain the evolutions of C_3H_6 and C_3H_8.

In any case, the quantum yield of H atom production in the photolysis of CH_4 has been measured directly at 121.6 nm as (0.47 ± 0.11) [20], and recent measurements have shown that the formation of CH_3 is an important process at this wavelength [21]. Although the quantum yields are likely to change somewhat as a function of wavelength, it is unlikely that the production of H atoms would drop significantly over only 2 nm.

4.1.3. Model C

Thus, we have investigated whether there may be a loss mechanism for H atoms missing from our standard model. In Model C, we have simply added a removal term for H atoms of 40 s^{-1}, corresponding to an experimental wall effect. It is quite likely that there were some wall effects in the experiment of Hellner, and including a simple description of this in our model does improve somewhat on our standard model. But model C does not explain the observations as well as Models A and B. However, a slightly slower rate of removal of H atoms would improve the overall fit with the data for all compounds except C_2H_2.

Therefore, it seems that, at 300 K, the changes made in the three models A, B and C all improve our standard model, although no one among them is sufficient to explain all the experimental data. At 77 K, there is little difference between the H concentrations in the models based on the schemes of Yung, Toublanc and ours. In addition, the H atom plays a much less important role as the rate constants for $C_2H_4 + H$ and $C_2H_2 + H$ are much smaller. So, the three changes made in Models A, B and C at 300 K have little impact on the concentration profiles calculated at 77 K.

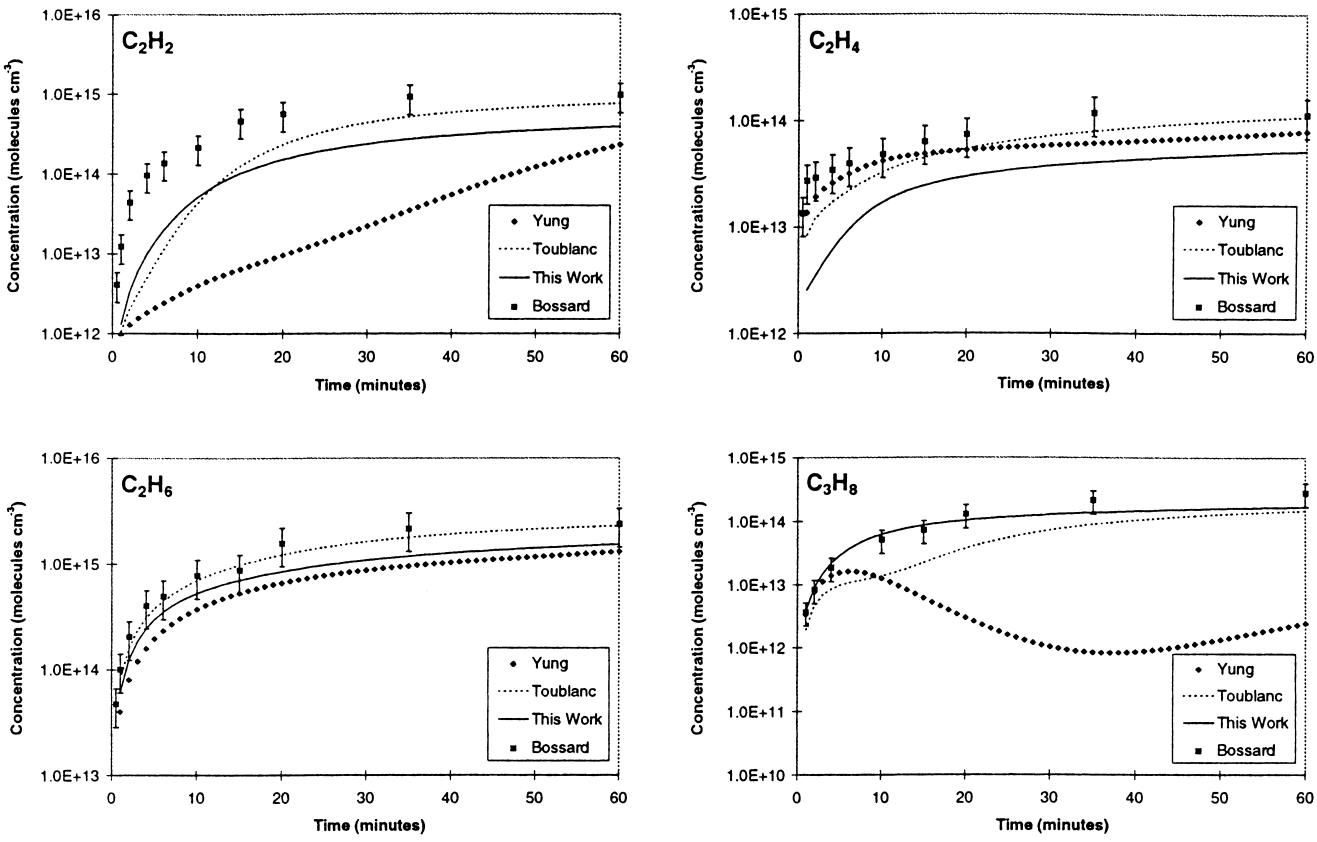

Fig. 4. Comparison of Bossard's results at 300 K (with error bars) with the photochemical schemes of Yung, Toublanc and our own model.

Our chemical scheme appears to describe the direct photolysis of CH_4 well, except for perhaps overpredicting the concentration of H atoms. On account of the three-body nature and temperature dependence of many reactions of H atoms, this overestimation of the concentration of H atoms appears unimportant at low temperatures and, more importantly, at low pressures. Although we need to further refine our scheme to reproduce all of the laboratory results above, our chemical scheme can be used, with confidence, to model methane photochemistry in cold or low pressure environments such as the atmosphere of Titan or interstellar clouds.

4.2. CH_4 photolysis at 147 nm

The photolysis of 9 Torr of CH_4 at 147 nm has been recently modelled by Dobrijevic [18]. He concluded that the chemical scheme of Toublanc explained Bossard's experimental results well for the C_2 species, but greatly overpredicted the quantities of C_3H_4, C_3H_6 and C_4H_4. We have also modelled this room-temperature experiment, using the chemical schemes of Yung, Toublanc and our own standard model. Bossard performed experiments at 6 and 9 Torr, and we have assumed that the same mechanisms operate at the two pressures. Thus, we have simply multiplied his concentrations at 6 Torr by a factor of 1.5 to create a composite data set, which is compared to our model results in Fig. 4. As no error bars were published with the experimental data, we have again assumed an uncertainty of 40%, as for Hellner's results, as both used gas chromatography for product quantification.

Similar to the photolysis at 123.6 nm, the models of Yung and Toublanc fit the data for C_2H_4 better than our model and all three models fail to reproduce the C_2H_2 evolution. Our results agree with the conclusion of Dobrijevic, that the chemical scheme of Toublanc gives, overall, a good agreement with the experimental data of Bossard for C_2H_4 and C_2H_6. We must also agree that this model, as well as that of Yung, predict very large amounts of C_3H_4 isomers, second in concentration only to C_2H_6, while Bossard only detected very small quantities, perhaps a concentration ten times lower than that of C_3H_6. Our model can explain this observation, and a comparison of C_3H_4 concentrations for the three different chemical schemes is shown in Table 1.

At 147 nm, methane only absorbs very weakly, and we have assumed an absorption cross section of 1×10^{-20} cm^2, as did Dobrijevic. This means that more strongly absorbing species, once produced, will also be photolysed, leading to a much more complicated series of chemical transformations. Only a fraction of the photons are absorbed by the mixture, and although CH_4 starts as the main absorbing species, after 20 min most photons lead to dissociation of C_2H_2. This produces the radicals C_2H or C_2, both of which can react with CH_4 to reform C_2H_2, which can be said to catalyse the

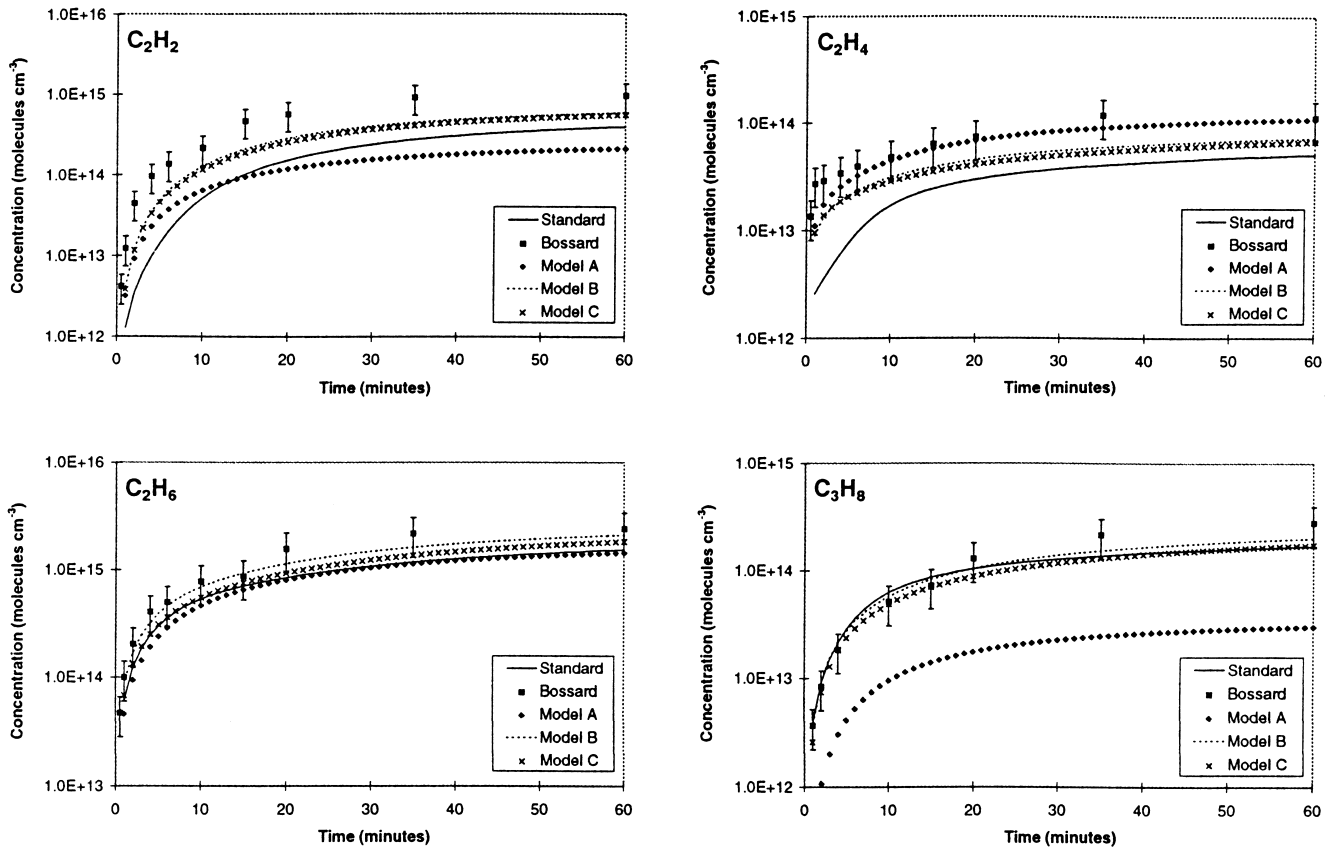

Fig. 5. Comparison of our models A, B and C (see text for details) with our standard model and the experimental data of Bossard (with error bars).

dissociation of CH_4 [22,23]. In the photolysis at 147 nm, both direct and C_2H_2-catalysed dissociation of CH_4 are in competition and, after 60 min of irradiation, the integrated rates for these two processes are, respectively, 1.44 and 1.49×10^{12} cm^{-3} s^{-1}.

We have also adapted our models A, B and C, as described above, to the experimental conditions of Bossard's 147 nm photolysis experiment, and we compare the results of our models with the experimental data in Fig. 5. The assumption of model A, that the rate constant of $C_2H_4 + H$ is 100 times smaller than the literature value is highly unlikely. A lower value for this rate constant diminishes the formation of C_2H_5 radicals, which, by recombination with CH_3, are the most important source of C_3H_8. Model A fails to explain the C_3H_8 evolution observed experimentally. Both, models B and C slightly improve our fit with the experimental data, but it is difficult to distinguish which is most likely the real case. As the quantum yield of H production has only been measured at 121.6 nm and is likely to vary as a function of wavelength, it may be significantly different, and even zero as assumed in model B, at 147 nm. On the other hand, loss of H atoms on the walls of the experimental reaction chamber is likely and explains the results equally well.

5. Conclusion

In summary, although our model has trouble reproducing the results of the 123.6 nm photolysis of CH_4 at 300 K, it appears fairly trustworthy under conditions of low temperature, low pressure and photolysis at 147 nm. In addition, it is the first photochemical scheme that can explain the low levels of C_3H_4 isomers formed in all these experiments. There is a reasonable possibility that the experiments we have performed suffered from some H loss processes on the reaction cell walls, as the fit between model and experiment improves when such a process is included in our model. As the two experiments we have investigated were performed in different reactors with different surface areas, it is unlikely that the H loss rate through wall effects would be the same. From our modelling it seems as though the H atom loss rate in Hellner's experiments was slightly less than 40 s^{-1}, while in Bossard's experiments, it was somewhat greater than 40 s^{-1}. If we assume that this wall effect is the main cause of the discrepancy between the model and the two sets of experimental data, our models still underestimate the concentrations of C_2H_2. If there is adsorption of H atoms, we may also expect adsorption of other radicals. Perhaps including such heterogeneous losses in our model would further improve our fit to the experimental data. However, in these systems only CH_3 and C_2H_5 radicals have concentrations comparable to H atoms and could possibly have equally significant wall effects. It is unlikely that a change in concentration of either of these radicals would strongly influence the concentration of C_2H_2. This suggests that there may be some production mechanism for this compound that is missing from our chemical scheme, or a loss mechanism that is overestimated.

The fact that the hypothesis of Model B improves the agreement between our theoretical calculations and the experimental results of Hellner and Bossard highlights the need for measurements of the photolysis parameters of CH_4. Accurate information on both the absorption cross section and quantum yields of this compound are required as a function of wavelength and of temperature [15]. With this data our comparison between model and experiment for the photolysis of CH_4 at 123.6 and 147 nm could yield more information about the possible presence of wall effects in these experiments. In this way, we would be able to propose a more robust chemical scheme, valid under any conditions of temperature, pressure and photolysis wavelength. The development of such a scheme is essential if we are to construct reliable photochemical models of the atmospheres of the giant planets, Titan and the interstellar medium.

Appendix A. Details of kinetic data used

Comparison of the three schemes

Table A.1. Absorption cross sections

Photolysis	Abs cx (123.6 nm)	Abs cx (147 nm)	Refs
CH_4	1.93E-17	1.00E-20	[18,19]
C_2H_2	7.31E-18	2.15E-17	[24]
C_2H_4	2.96E-17	1.60E-17	[25]
C_2H_6	2.15E-17	1.40E-18	[19]
CH_3C_2H (MA)	7.31E-17	1.80E-17	[24]
CH_2CCH_2 (ALL)	5.20E-17	2.60E-17	[26]
C_3H_6	4.26E-17	2.20E-17	[27]
C_3H_8	3.33E-17	6.10E-18	[19]
C_4H_2	2.63E-17	2.60E-17	[28]
C_4H_4	2.63E-17	2.60E-17	assumed same values as C_4H_2

In the absence of data, the absorption cross section of C_4H_4 was assumed equal to that of C_4H_2.

Table A.2. Quantum yields

Photolysis	P1	P2	P3	Toublanc	Yung	This work	Refs.
CH_4	CH_3	H		—	—	0.41	[15]
	$1CH_2$	H_2		1.00	1.00	0.53	
	CH	H_2	H	—	—	0.06	
C_2H_2	C_2H	H		0.30	0.06	0.30	[28]
	C_2	H_2		0.10	0.10	0.10	
C_2H_4	C_2H_2	H_2		0.5	10.5	10.50	[29]
	C_2H_2	H	H	0.49	0.49	0.50	
C_2H_6	C_2H_4	H_2		0.56	0.56	0.56	[30]
	C_2H_4	H	H	0.14	0.14	0.13	
	C_2H_2	H_2	H_2	0.27	0.27	0.29	
	CH_4	$1CH_2$		0.02	0.02	0.02	
	CH_3	CH_3		0.01	0.01	—	
CH_3C_2H (MA)	C_3H_3	H		0.40	0.40	0.40	[31]
	C_3H_2	H_2		0.15	0.15	0.15	
	C_2H	CH_3		0.02	0.02	—	
CH_2CCH_2 (ALL)	C_3H_3	H		0.40	0.40	0.89	[32]
	C_3H_2	H_2		0.15	0.15	0.11	
	C_2H_2	$3CH_2$	0.06	0.06	0.06		
C_3H_6	ALL	H	H	—	—	0.23	[33,34]
	ALL	H_2		0.57	0.57		
	MA	H	H	—	—	0.12	
	C_2H_3	CH_3		—	—	0.25	
	C_2H_2	CH_3	H	0.34	0.34	—	
	C_2H_4	$3CH_2$		0.02	0.02	0.05	
	C_2H_2	CH_4		—	—	0.05	
	C_2H	CH_4	H	0.05	0.05	—	
C_3H_8	C_3H_6	H_2		0.94	0.94	0.94	[4]
	C_2H_4	CH_4		0.06	0.06	0.06	
C_4H_2	C_4H	H		0.20	0.30	0.20	[35]
	C_2H_2	C_2		0.10	—	0.10	
	C_2H	C_2H		0.03	0.30	0.03	
	$C_4H_2^{**}$			0.67	—	—	
C_4H_4	C_4H_2	H_2		1.00	1.00	1.00	Assumed

All quantum yields were assumed to be the same at 123.6 and 147 nm due to the absence of data as a function of wavelength. The total quantum yield of C_4H_4 was assumed to be 1.

Table A.3. Rate constants

Reaction	R1	R2		P1	P2	Toublanc	Yung	This work	Refs.
R0101	H	H	→	H_2		2.98E-15			
R01T12a	H	$3CH_2$	→	CH	H_2			2.01E-10	[8]
R01T12b	H	$3CH_2$	→	CH_3		4.69E-12			
R0113	H	CH_3	→	CH_4		4.42E-11	1.18E-10	1.85E-11	[8]
R0121	H	C_2H	→	C_2H_2		7.86E-10			
R0122	H	C_2H_2	→	C_2H_3		5.97E-14	3.42E-14	6.15E-14	[8]
R0123	H	C_2H_3	→	C_2H_2	H2	2.00E-11	1.50E-11	2.00E-11	[8]

Table A.3. (*Continued*)

Reaction	R1	R2		P1	P2	Toublanc	Yung	This work	Refs.
R0124	H	C_2H_4	→	C_2H_5		4.34E-13	6.02E-13	4.37E-13	[8]
R0125	H	C_2H_5	→	CH_3	CH_3	5.21E-11	4.38E-11	6.00E-11	[8]
R0132	H	C_3H_2	→	C_3H_3		1.78E-11	1.46E-10	1.00E-10	[36]
R0133a	H	C_3H_3	→	MA		1.78E-11	1.46E-10	2.50E-11	[36]
R0133b	H	C_3H_3	→	ALL		1.78E-11	1.46E-10	2.50E-11	[36]
R01A34a	H	ALL	→	C_2H_2	CH_3	5.47E-15	5.47E-15		
R01A34b	H	ALL	→	C_3H_5		2.48E-13	2.48E-13	1.27E-13	see below
R01A34x	H	ALL	→	MA	H	2.74E-13	3.57E-13		
R01M34a	H	MA	→	C_2H_2	CH_3	4.98E-14	4.98E-14		
R01M34b	H	MA	→	C_3H_5		4.98E-14	4.98E-14	1.27E-13	[37,38]
R0135a	H	C_3H_5	→	MA	H_2	3.30E-10	1.50E-11	1.50E-11	[8]
R0135b	H	C_3H_5	→	ALL	H_2	3.00E-11	1.50E-11	1.50E-11	[8]
R0135c	H	C_3H_5	→	C_2H_3	CH_3			1.82E-11	[8]
R0135d	H	C_3H_5	→	C_2H_2	CH_4	3.30E-10	1.50E-11		
R0135e	H	C_3H_5	→	C_3H_6		7.67E-12	7.67E-12		
R0136	H	C_3H_6	→	C_3H_7		9.37E-13	9.37E-13	9.13E-13	[37]; see below
R0137	H	C_3H_7	→	C_2H_5	CH_3	4.33E-28	4.38E-11	6.00E-11	see below
R0141	H	C_4H	→	C_4H_2		2.62E-10			
R0142	H	C_4H_2	→	C_4H_3		2.69E-12		8.93E-14	[39]; see below
R0143a	H	C_4H_3	→	C_4H_2	H_2	1.20E-11	1.20E-11	1.20E-11	[4]
R0143b	H	C_4H_3	→	C_2H_2	C_2H_2	3.30E-12	3.30E-12	3.30E-12	[4]
R0143c	H	C_4H_3	→	C_4H_4		2.22E-10	3.30E-12	1.79E-11	[40]
R1102	CH	H_2	→	CH_3				7.26E-13	[8]
R1114	CH	CH_4	→	C_2H_4	H		1.00E-10	9.74E-11	[8]
R1122	CH	C_2H_2	→	C_3H_2	H			4.29E-10	[8]
R1124	CH	C_2H_4	→	ALL/MA	H			3.92E-10	[8]
R1126	CH	C_2H_6	→	C_3H_6	H			2.79E-10	[8]
R1138	CH	C_3H_8	→	SOOT	H			4.23E-10	[8]
RS1202	$1CH_2$	H_2	→	CH_3	H	1.20E-10	7.00E-12	1.20E-10	[8]
RS1214	$1CH_2$	CH_4	→	CH_3	CH_3	5.90E-11	1.90E-12	7.10E-11	[9]
RS1222	$1CH_2$	C_2H_2	→	C_3H_3	H			2.90E-10	[8]
RS1224	$1CH_2$	C_2H_4	→	C_3H_6				1.60E-10	[8]
RS1226	$1CH_2$	C_2H_6	→	C_2H_5	CH_3			1.90E-10	[9]
RT12T12	$3CH_2$	$3CH_2$	→	C_2H_2	H_2	5.30E-11	5.30E-11	5.27E-11	[8]
RT1213	$3CH_2$	CH_3	→	C_2H_4	H	7.00E-11	7.00E-11	7.00E-11	[8]
RT1222a	$3CH_2$	C_2H_2	→	MA		3.34E-16	2.20E-12	1.51E-16	[8]
RT1222b	$3CH_2$	C_2H_2	→	ALL		5.80E-12	3.70E-12	1.51E-16	[8]
RT1223	$3CH_2$	C_2H_3	→	C_2H_2	CH_3			3.00E-11	[9]
RT1224	$3CH_2$	C_2H_4	→	C_3H_5	H			7.47E-16	[8]
RT1225	$3CH_2$	C_2H_5	→	C_2H_4	CH_3			3.00E-11	[9]
RT1238	$3CH_2$	C_3H_8	→	C_3H_7	CH_3			1.22E-16	[41]
R1313	CH_3	CH_3	→	C_2H_6		5.49E-11	5.50E-11	5.93E-11	[8]
R1323a	CH_3	C_2H_3	→	C_2H_2	CH_4	3.40E-11	9.10E-12	6.50E-13	[9]
R1323b	CH_3	C_2H_3	→	C_3H_6		1.20E-10	9.10E-12	4.17E-11	[8]
R1325a	CH_3	C_2H_5	→	C_2H_4	CH_4	1.88E-12	8.73E-13	1.90E-12	[8]
R1325b	CH_3	C_2H_5	→	C_3H_8		2.16E-11	2.16E-11	5.60E-11	[8]
R1335a	CH_3	C_3H_5	→	ALL	CH_4	6.50E-11	4.50E-12	3.50E-13	[8]
R1335b	CH_3	C_3H_5	→	MA	CH_4	6.50E-11	4.50E-12		
R1335c	CH_3	C_3H_5	→	SOOT				3.39E-11	[8]
R1337a	CH_3	C_3H_7	→	C_3H_6	CH_4	3.06E-12	1.28E-12	5.60E-11	[37]; see below
R1337b	CH_3	C_3H_7	→	SOOT		5.16E-11	2.16E-11		
R2002	C_2	H_2	→	C_2H	H	1.32E-12	1.40E-12	1.32E-12	[42]

Table A.3. (*Continued*)

Reaction	R1	R2		P1	P2	Toublanc	Yung	This work	Refs.
R2014	C_2	CH_4	→	C_2H	CH_3	2.04E-11	1.90E-11	2.04E-11	[42]
R2102	C_2H	H_2	→	C_2H_2	H	1.38E-13	1.51E-13	4.76E-13	[8]
R2114	C_2H	CH_4	→	C_2H_2	CH_3	1.30E-12	1.22E-12	3.00E-12	[8]
R2122	C_2H	C_2H_2	→	C_4H_2	H	1.38E-10	3.10E-11	1.50E-10	[8]
R2124	C_2H	C_2H_4	→	C_4H_4	H	2.50E-11		2.00E-11	[9]
R2126	C_2H	C_2H_6	→	C_2H_5	C_2H_2	3.60E-11	6.50E-12	6.00E-12	[9]
R2138	C_2H	C_3H_8	→	C_3H_7	C_2H_2	6.00E-12	1.40E-11	7.88E-11	[43]
R2142	C_2H	C_4H_2	→	POLYYNES	H	4.15E-11	3.10E-11	1.50E-10	[44]
R2302	C_2H_3	H_2	→	C_2H_4	H	9.83E-20			
R2323a	C_2H_3	C_2H_3	→	C_2H_4	C_2H_2	2.40E-11	5.30E-12	1.60E-12	[9]
R2323b	$C_2H_3C_2$	H_3	→	SOOT		1.20E-10		1.60E-11	[9]
R2325a	C_2H_3	C_2H_5	→	C_2H_4	C_2H_4	3.00E-12	3.00E-12	8.00E-13	[9]
R2325b	C_2H_3	C_2H_5	→	C_2H_6	C_2H_2	6.00E-12	6.00E-12	8.00E-13	[9]
R2325c	C_2H_3	C_2H_5	→	SOOT				2.49E-11	[9]
R2525a	C_2H_5	C_2H_5	→	C_2H_6	C_2H_4	1.98E-12	1.26E-12	2.40E-12	[8]
R2525b	C_2H_5	C_2H_5	→	SOOT		9.47E-12	9.47E-12	1.90E-11	[8]
R3333	C_3H_3	C_3H_3	→	SOOT				1.17E-10	[45]
R3535a	C_3H_5	C_3H_5	→	C_3H_6	ALL			1.55E-13	[8]
R3535b	C_3H_5	C_3H_5	→	SOOT				2.63E-11	[8]
R3737a	C_3H_7	C_3H_7	→	C_3H_8	C_3H_6			4.20E-12	[8]
R3737b	C_3H_7	C_3H_7	→	SOOT				6.80E-12	[8]
R4102	C_4H	H_2	→	C_4H_2	H	1.55E-13		4.76E-13	see below
R4114	C_4H	CH_4	→	C_4H_2	CH_3	4.35E-13	4.04E-13	3.00E-12	see below
R4122	C_4H	C_2H_2	→	POLYYNES	H	4.57E-11	1.00E-11	1.50E-10	see below
R4124	C_4H	C_2H_4	→	SOOT	H	1.20E-11		2.00E-11	see below
R4126	C_4H	C_2H_6	→	C_4H_2	C_2H_5	1.20E-11	2.20E-12	6.00E-12	see below
R4138	C_4H	C_3H_8	→	C_4H_2	C_3H_7			7.88E-11	see below
R4142	C_4H	C_4H_2	→	POLYYNES	H	5.81E-11	1.00E-11	1.50E-10	see below
R4200	C_4H_2b		→	C_4H_2		1000			
R4242	C_4H_2b	C_4H_2	→	POLYYNES	H_2	1.47E-10			

All values are the effective bimolecular rate constants ($cm^3\ s^{-1}$) calculated for a temperature of 300 K and a pressure of 10 Torr. For three-body reactions, we use either $k = k_0 \times M$, in the absence of a k_∞ value, or in preference the expression

$$k = \frac{k_0 \times k_\infty \times M}{(k_\infty + (k_0 \times M))}$$

We have had to estimate the unknown k_0 values for certain reactions. We have, therefore, equated the following pairs of k_0 values: R0136 with R0124, R0142 with R0122, R0143 with R0123, and R1337a with R1325b. We have also had to assume that the rate constants of R01A34b and R0137 are the same as those for R01M34b and R0125, respectively. All the reactions of C_4H are assumed to have the same rates as the equivalent reactions of C_2H.

References

[1] G.R. Gladstone, M. Allen, Y.L. Yung, Icarus 119 (1996) 1.
[2] S.K. Atreya, T. Encrenaz, H. Feuchtgruber, S.G. Edgington, Bull. American Astron. Soc., DPS Meeting #30, #26.03(1998).
[3] Y.L. Yung, Icarus 72 (1987) 468.
[4] Y.L. Yung, M. Allen, J.P. Pinto, Astrophys. J. Supp. Ser. 55 (1984) 465.
[5] D. Toublanc, J.P. Parisot, J. Brillet, D. Gautier, F. Raulin, C.P. McKay, Icarus 113 (1995) 2.
[6] L. Lara, E. Lellouch, J.J. Lopez-Moreno, R. Rodrigo, J. Geophys. Res. 101 (1996) 23261.
[7] D.L. Baulch, C.J. Cobbs, R.A. Cox, C. Esser, P. Frank, T. Just, J.A. Kerr, M.J. Pilling, J. Troe, R.W. Walker, J. Warnatz, J. Phys. Chem. Ref. Data 21 (1992) 411.
[8] D.L. Baulch, C.J. Cobbs, R.A. Cox, C. Esser, P. Frank, T. Just, J.A. Kerr, M.J. Pilling, J. Troe, R.W. Walker, J. Warnatz, J. Phys. Chem. Ref. Data 23 (1994) 847.
[9] W. Tsang, R.F. Hampson, J. Phys. Chem. Ref. Data 15 (1986) 1087.
[10] W. Tsang, J. Phys. Chem. Ref. Data 17 (1988) 887.
[11] W. Tsang, J. Phys. Chem. Ref. Data 20 (1991) 221.
[12] J. Warnatz, in W.C. Gardiner (Ed.), Combustion Chemistry. Rate coefficients in the C/H/O system, Springer-Verlag, New York, 1984, p. 197.
[13] L. Hellner, Thse, Facult des Sciences de Paris, 1969.

[14] A. Bossard, Thse, Universit Paris VI, 1979.
[15] N.S. Smith, F. Raulin, J. Geophys. Res. 104 (1999) 1873.
[16] T.G. Slanger, G. Black, J. Chem. Phys. 77 (1982) 2432.
[17] A.R. Curtis, The FACSIMILE numerical integrator for stiff initial value problems, United Kingdom Atomic Energy Authority, Harwell, Oxfordshire, 1979.
[18] M. Dobrijevic, J.P. Parisot, Adv. Space Res. 15 (1995) 1.
[19] J.G. Calvert, J.N. Pitts, Photochemistry, Wiley, New York, 1966.
[20] R.A. Brownsword, M. Hillenkamp, T. Laurent, R.K. Vatsa, H.R. Volpp, J. Wolfrum, Chem. Phys. Lett. 266 (1997) 259.
[21] D.H. Mordaunt, I.R. Lambert, G.P. Morley, M.N.R. Ashfold, R.N. Dixon, C.M. Western, L. Schnieder, K.H. Welge, J. Chem. Phys. 98 (1993) 2054.
[22] N.S. Smith, M.-C. Gazeau, A. Khelifi, F. Raulin, Planet. Space Sci. 47 (1999) 3.
[23] Y.L. Yung, D.F. Strobel, Astrophys. J. 239 (1980) 395.
[24] T. Nakayama, K. Watanabe, J. Chem. Phys. 40 (1964) 558.
[25] M. Zelikoff, K. Watanabe, J. Opt. Soc. Am. 43 (1953) 756.
[26] J.W. Rabalais, J.M. McDonald, V. Scherr, S.P. McGlynn, Chem. Rev. 71 (1971) 73.
[27] J.A.R. Samson, F.F. Marmo, K. Watanbe, J. Chem. Phys. 36 (1962) 783.
[28] H. Okabe, J. Chem. Phys. 75 (1981) 2772.
[29] R.A. Back, D.W.L. Griffiths, J. Chem. Phys. 46 (1967) 4839.
[30] R.F. Hampson Jr., J.R. McNesby, J. Chem. Phys. 42 (1965) 2200.
[31] L.J. Stief, V.J. DeCarlo, W.A. Payne, J. Chem. Phys. 54 (1971) 1913.
[32] W.M. Jackson, D.S. Anex, R.E. Continetti, B.A. Balko, Y.T. Lee, J. Chem. Phys. 95 (1991) 7327.
[33] T. Gierczak, J. Gawlowski, J.N. Niedzielski, J. Photochem. Photobiol. A. Chem. 43 (1988) 1.
[34] J. Niedzielski, W. Makulski, J. Gawlowski, J. Photochem. 19 (1982) 123.
[35] S. Glicker, H. Okabe, J. Phys. Chem. 91 (1987) 437.
[36] J. Peeters, Int. J. Chem. Kinet. 26 (1994) 869.
[37] A.H. Laufer, E.P. Gardner, T.L. Kwok, Y.L. Yung, Icarus 56 (1983) 560.
[38] D.A. Whytock, W.A. Payne, L.J. Stief, J. Chem. Phys. 65 (1976) 191.
[39] D.F. Nava, M.B. Mitchell, L.J. Stief, J. Geophys. Res. 91 (1986) 4585.
[40] R. Duran, J. Phys. Chem. 92 (1988) 636.
[41] T. Bohland, S. Dobe, F. Temps, H.G. Wagner, Ber. Bunsen-Ges. Phys. Chem. 89 (1985) 1110.
[42] W.M. Pitts, Chem. Phys. 68 (1982) 417.
[43] R.J. Hoobler, B.J. Opansky, S.R. Leone, J. Phys. Chem. A 101 (1997) 1338.
[44] H. Brachhold, U. Alkemade, K.H. Homann, Ber. Bunsen-Ges. Phys. Chem. 92 (1988) 916.
[45] C.L. Morter, S.K. Farhat, D.J. Adamson, G.P. Glass, R.F. Curl, J. Phys. Chem. 98 (1994) 7029.